



Comparative electrochemical investigations on series of SH-terminated-functional porphyrins

Wenting Wang^{a,b}, Yaqi Hu^b, Chunming Wang^{a,*}, Xiaoquan Lu^{b,**}

^a College of Chemistry and Chemical Engineering, Lanzhou University, Lanzhou 730000, China

^b Key Laboratory of Bioelectrochemistry & Environmental Analysis of Gansu Province, College of Chemistry & Chemical Engineering, Northwest Normal University, Lanzhou 730070, China

ARTICLE INFO

Article history:

Received 30 November 2011

Received in revised form 12 January 2012

Accepted 13 January 2012

Available online 21 January 2012

Keywords:

SH-terminated porphyrins

Alkanethiols

Electron transfer (ET) kinetics

Scanning electrochemical microscopy

(SECM)

Density functional theory (DFT)

ABSTRACT

The electrochemical behaviors of self-assembled substituted porphyrins (SH-terminated, abbreviated as $H_2TPPO(CH_2)_nSH$, $n = 3, 12$) on a gold electrode were investigated using the steady-state scanning electrochemical microscopy (SECM). The different electron-transfer (ET) kinetics, including the bimolecular ET between the porphyrin self-assembled monolayers (SAMs) and the redox mediator $[K_3Fe(CN)_6]$, the tunneling ET between the underlying gold electrode and $[K_3Fe(CN)_6]$, and pinholes or defects, were clearly distinguishable. The SECM strategy was developed to deal with the two types of porphyrin SAMs. First, a model using alkanethiols $[(CH_2)_nSH, n = 3, 12]$ as the functional template was proposed to change the conformation of porphyrin SAMs in a unit area of the electrode. Second, the porphyrin SAMs were directly prepared by inserting a metal (cobalt) into the center of the porphyrin ring. The results show the distinct effect of the presence of alkanethiols on the kinetics of the different-chain length porphyrins. In addition, the rate constants of the bimolecular ET significantly increased after the insertion of cobalt. The results are in agreement with the density functional theory (DFT).

© 2012 Elsevier Ltd. All rights reserved.

1. Introduction

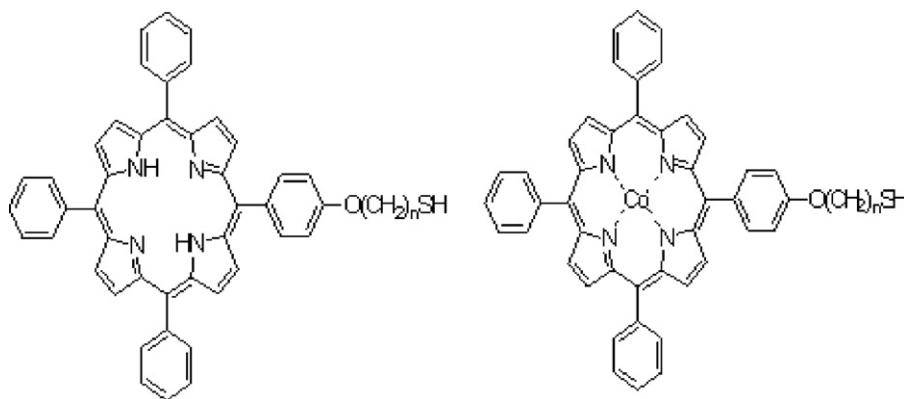
The electron-transfer (ET) process occurs in a wide variety of chemical and biological systems, and ET kinetics has been extensively studied in analytical electrochemistry. Porphyrin compounds, which are important biochemical molecules, were used in numerous applied studies, including those of catalysts, selective anion sensing and photocurrent catchers [1–4]. Several methods of the immobilization with porphyrins, such as the formation of self-assembled monolayers (SAMs) [5,6], covalent appended monolayers [7,8], and polymerization monolayers with the formation of an electroactive film [9,10] are available. Of these, SAMs can spontaneously form highly ordered monolayers and are extensively used [11]. Meanwhile, alkanethiols are widely used in the fabrication of SAMs, and result in improved stability and sensitivity of electrochemical biosensors [12]. The electrochemical properties of surfaces modified by alkanethiols were investigated, and the functionality of the surface was controlled through the generation of alkanethiol groups in SAMs [13,14]. The structure and

long-range electronic properties were also studied through the use of two kinds of alkanethiol monolayers containing amide bonds [15,16]. Given the advantages of alkanethiols in SAMs, their use as the functional template on a gold electrode was proposed. Porphyrins and metalloporphyrin derivatives such as snowflake-shaped porphyrin dendrites, porphyrins with axial carbazole-based dendritic substituents, and long-lived porphyrins can therefore be successfully constructed [17–19]. Co porphyrins, which are metalloporphyrin derivatives, were widely used as oxygen carriers to investigate the facilitated transport of oxygen [20]. The photo-electrochemical properties of electrodes modified using an ordered supramolecular assembly of porphyrins and the effect of the porphyrin substituent groups were investigated [21,22]. The steady-state scanning electrochemical microscopy (SECM), which provides a rapid identification of new dyes as well as the electrocatalytic activity of the metalloporphyrin-modified substrates with regard to the oxygen reduction reaction [23,24], has been extensively described [25–28]. Given the many advantages of SECM in observing the electrochemical reactions at the interfaces, it was widely used to mimic and study the chemical nature of interfaces [29–31]. The structure of porphyrin SAMs on the substrate affected the electron transfer process, and the alkyl chain length also influenced the ET kinetics of porphyrins via SECM [32,33]. Furthermore, the tilt-angles of porphyrins with different alkyl chains on the electrode were investigated [34]. The results showed that porphyrins

* Corresponding author. Tel.: +86 931 8912582; fax: +86 931 8912582.

** Corresponding author. Tel.: +86 931 7971276; fax: +86 931 7971276.

E-mail addresses: wangcm@lzu.cn (C. Wang), luxq@nwnu.edu.cn, taaluxq@gmail.com (X. Lu).



Scheme 1. The scheme of sulfhydryl porphyrins compounds ($\text{H}_2\text{TPPO}(\text{CH}_2)_n\text{SH}$ and $\text{Co-H}_2\text{TPPO}(\text{CH}_2)_n\text{SH}$).

with longer alkyl chains ($n=12$) can be almost perpendicular to the surface of the electrode, however, porphyrins with short alkyl chains ($n=3$) are evenly distributed on the surface of the electrode. Based on the previous work, two types of systems were designed to investigate the factors affecting the ET kinetics of porphyrins on the electrode. First, alkanethiols $[(\text{CH}_2)_n\text{SH}, n=3, 12]$ as a functional template was proposed to change the porphyrin SAMs in a unit area on the electrode. Second, porphyrin SAMs without alkanethiols were metalized with Co ions in the center of the porphyrin ring. Using the SECM technique, the three ET pathways, which were bimolecular ET between porphyrin SAMs and the redox mediator [ferricyanide, $\text{K}_3\text{Fe}(\text{CN})_6$], the tunneling ET between the underlying gold electrode and $[\text{K}_3\text{Fe}(\text{CN})_6]$ and the pinholes or defects were clearly distinguishable. The corresponding ET rate constants were then obtained. In addition, the density functional theory (DFT) was applied to support the experimental results.

2. Experimental

2.1. Chemicals and reagents

Sulfhydryl porphyrins compounds (abbreviated as $\text{H}_2\text{TPPO}(\text{CH}_2)_n\text{SH}$, $n=3, 12$) were synthesized by the previous reported methodology [35] and characterized by UV-Vis, IR and ^1H NMR (see Supporting Information), and Co-porphyrins was prepared using the methods reported by Nishimura et al. (the structure is shown in Scheme 1) [36]. Alkanethiols $[(\text{CH}_2)_n\text{SH}, n=3, 12]$ were used as received from Alfa Aesar (China(Tianjin) Co., Ltd). All other reagents were analytical-reagent grade, unless otherwise specified. Solutions were prepared from water that had been purified through an Ultra-pure water system Milli-Q Plus (Millipore).

2.2. Apparatus

Electrochemical experiments were carried out using a CHI 900 scanning electrochemical microscope (CH Instruments Co. Ltd., Austin, USA) with a four-electrode cell. The gold (or modified gold) electrode, a platinum wire, and a KCl saturated Ag/AgCl electrode were used as working, counter and reference electrode, respectively. The SECM tip was a 25- μm diameter Pt ultramicroelectrode (UME). Before each experiment, the tip was polished with 0.3- μm alumina and rinsed with DI water, and the solutions were purged with pure nitrogen for 15 min before each run.

2.3. Preparation of substrate and SAMs

A gold electrode was used as the substrate. The electrode was polished to a mirror finish using 0.05 μm alumina powder before

careful rinsing with deionized (DI) water, sonication in absolute ethanol and DI water for 10 min in turn, and then dried with nitrogen gas. SAMs was prepared with a solution of 1 mM alkanethiols in ethanol, and then put in 1 mM sulfhydryl porphyrins compounds in chloroform for 24 h. SAMs with sulfhydryl Co-porphyrins compounds were prepared with a solution of 1 mM sulfhydryl porphyrins compounds in chloroform for 24 h and then metalized with cobalt ion. During the self-assembled process, the electrode was disposed in solution of chloroform or ethanol and DI water in turn with ultrasonic instrument every 3 h to remove the physical adsorption.

3. Results and discussion

In the current paper, the electron-transfer (ET) kinetics of the porphyrin self-assembled monolayers (SAMs) using the steady-state SECM in unbiased conditions was based on the heterogeneous rate constant (k_{eff}). SECM is an electrochemical approach to scanning probe microscopy with a good resolution. In steady-state SECM, an electrochemical redox cycle between the substrate (electrode) and the 25- μm diameter ultramicroelectrode (UME) tip occurs. The tip currents (i_T), are all divided by the steady-state current ($i_{T,\infty}$). $i_T/i_{T,\infty}$ is called normalized current (I_{norm}), and $i_{T,\infty}$ is expressed in the following equation:

$$i = 4nFDca \quad (1)$$

where n is the number of electrons transferred per molecule, F is the Faraday constant, D is the diffusion coefficient of the electroactive molecule, c is the bulk concentration of the electroactive molecule, and a is the radius of the tip [37]. The tip current (i_T) is expressed as follows:

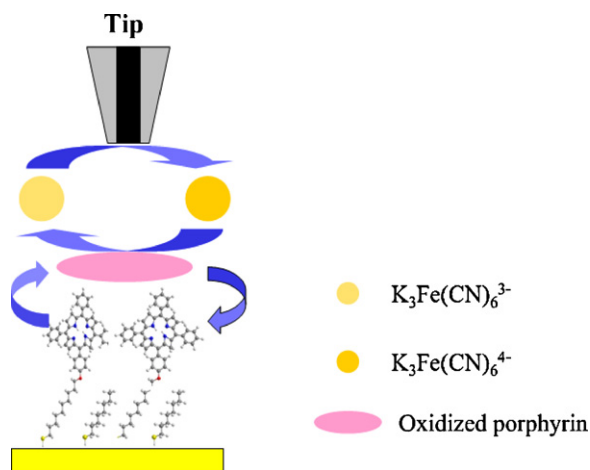
$$I_T^k - I_S^k \left(1 - \frac{I_T^{\text{ins}}}{I_T^{\text{c}}} \right) + I_T^{\text{ins}} \quad (2)$$

$$I_S^k = \frac{0.78377}{L(1+1/\Lambda)} + \frac{0.68 + 0.3315 \exp(-1.0672/L)}{1 + (11/\Lambda + 7.3)/(110 - 40L)} \quad (3)$$

where I_T^{c} and I_T^{ins} are the tip currents of the conductive and insulating substrates, respectively. In the current study, the substrate with the porphyrin compounds is a conductor, and the I_T^{c} is expressed in the following equation:

$$I_T^{\text{c}} = 0.68 + \frac{0.78377}{L} + 0.3315 \exp\left(-\frac{1.0672}{L}\right) \quad (4)$$

where $\Lambda = k_{\text{eff}}d/D$ (k_{eff} is equal to the apparent heterogeneous rate constant (cm s^{-1}) obtained using the experimental probe approach curves that fit the theoretical data, and D is the diffusion coefficient). $L = d/a$, where L is the distance between the normalized tip electrode

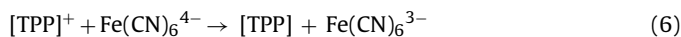


Scheme 2. The mode on SECM system of porphyrins with the templates of alkanethiols on the gold electrode.

and the substrate, d is the distance between the tip electrode and the substrate and a is the radius of the tip electrode. I_T^k , I_T^c and I_T^{ins} are normalized by the tip current at an infinite tip–substrate distance [38,39].

In Scheme 2, $\text{K}_3\text{Fe}(\text{CN})_6$ was chosen as the reversible redox couple, the substrate was the porphyrin SAMs, and alkanethiols were used as the template on the gold electrode in the SECM electrochemical cell.

By controlling the substrate potential (E_s), redox reactions occur at the interfaces with porphyrins (TPP) as follows:



Given that the reaction in Eq. (6) is not reversible and that in Eq. (5) is quasi-reversible, k_{eff} is expressed as

$$k_{\text{eff}} = \frac{k_{\text{ox}} k_b \Gamma^*}{k_{\text{ox}} c^0 + k_b + k_f} + k' \quad (7)$$

where c^0 is the concentration of the redox mediator, k_{ox} is the bimolecular oxidation rate constant, k_b is the tunneling rate constant, and k' is the defects and pinholes rate constant. For SAMs with different chain lengths, the ET between the substrate and the redox species was measured using the newly developed SECM methodol-

ogy [40,41]. The values of k_{ox} for the short-chain SAMs ($n = 3$) could be calculated using Eq. (8), as follows:

$$\frac{\Gamma^*}{k_{\text{eff}} - k'} = \frac{c^0}{k_b} + \frac{1 + \exp[-F(E_s - E_{\text{ads}}^0)/RT]}{k_{\text{ox}}} \quad (8)$$

where E_{ads}^0 is the formal potential of the SAMs-bound redox species, Γ^* is the surface concentrations of oxidized and reduced forms of redox centers in the monolayers. Additionally, the values of k_{ox} can be calculated using the following equation for the long-chain SAMs ($n = 12$):

$$k_{\text{eff}} = k_{\text{ox}} \Gamma^* + k' \quad (9)$$

where E_s is much more negative than E_{ads}^0 . For k_b , the value for the rate constant can be calculated using the following equation:

$$k_{\text{eff}} = \frac{k_b \Gamma^*}{c^0} + k' \quad (10)$$

where E_s is relatively low and equal to E_{ads}^0 .

3.1. Electrochemical characterization of the formation of the self-assembled monolayers (SAMs)

Electrochemical measurements can provide valuable insights into the structure of a film on a substrate surface [5,42]. Cyclic voltammetry (CV) was used to determine the surface coverage (Γ) of porphyrin self-assembled monolayers (SAMs) through redox stripping at the negative potential (-0.9 V) according to the following equation:

$$\Gamma = \frac{Q}{nFA}$$

where Q is the peak area in coulombs, A is the electrode surface area, F is the Faraday constant and n is the number of electrons involved in the electrode interaction [43]. To further confirm the results, the hindrance (θ) of the electrode as a qualitative parameter of SAMs density was obtained using the following equation:

$$\theta = 1 - \left[\frac{i_p^f(\text{TPP})}{i_p^f(\text{Au})} \right]$$

where $i_p^f(\text{TPP})$ and $i_p^f(\text{Au})$ are the forward (reduction of ferricyanide) peak currents at the modified and bare electrodes, respectively. As representatives of the short-chain and long-chain SAMs, the porphyrins $[\text{H}_2\text{TPPO}(\text{CH}_2)_n\text{SH}]$, $n = 3, 12$ and the corresponding alkanethiols (as the functional template) were provided. Table 1

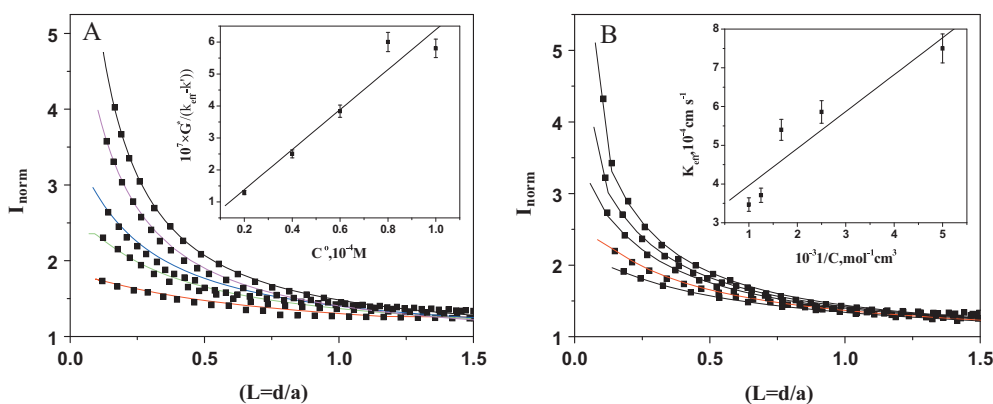
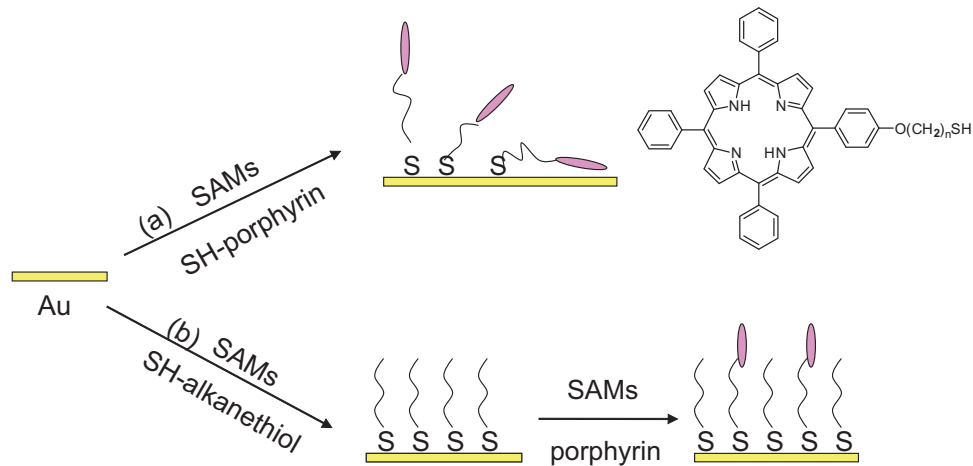


Fig. 1. (A) Probe approach curves (PACs) of $\text{H}_2\text{TPPO}(\text{CH}_2)_3\text{SH}$ ($n = 3$) with alkanethiols as the template (from bottom to top the concentration of $\text{K}_3\text{Fe}(\text{CN})_6$ are 0.2, 0.4, 0.6, 0.8, 1.0 mM). Inset: Dependence of the effective heterogeneous rate constants in 0.1 M KCl solution. (B) PACs of $\text{H}_2\text{TPPO}(\text{CH}_2)_{12}\text{SH}$ ($n = 12$) with alkanethiols as the template (from bottom to top the concentration of $\text{K}_3\text{Fe}(\text{CN})_6$ are 0.2, 0.4, 0.6, 0.8, 1.0 mM). Inset: Dependence of the effective heterogeneous rate constants. The diamonds are experimental PACs, lines are theoretical PACs.



Scheme 3. The scheme (a) porphyrins directly self-assembled on the substrate; (b) porphyrins self-assembled on the substrate of alkanethiols as the templates.

Table 1

Γ , θ and molecular area value of the functional porphyrins ($H_2TPPO(CH_2)_nSH$ ($n = 3, 12$)) at alkanethiols ($(CH_2)_nSH$, $n = 3, 12$) of the same chain length as the template with different self-assembled time.

| System | Parameter | Time (h) | | | |
|----------|---|----------|-------|-------|--------|
| | | 2 | 4 | 6 | 8 |
| $n = 3$ | Γ (pmol/cm ²) | 68 | 190 | 273 | 223 |
| | θ (%) | 34.36 | 38.69 | 29.02 | 6.6 |
| | Molecular area (Å ² molecule ⁻¹) | 245 | 84.75 | 74.49 | 60.85 |
| $n = 12$ | Γ (pmol/cm ²) | 262 | 452 | 274 | 64 |
| | θ (%) | 51.9 | 25.44 | 15.37 | 1.81 |
| | Molecular area (Å ² molecule ⁻¹) | 63.4 | 36.75 | 60.63 | 259.56 |

shows the Γ , θ and molecular area of the porphyrins with alkanethiols of the same alkyl chain length as the functional template at different self-assembly times. The calculated Γ is consistent with previous results [44,45]. When a porphyrin ring was considered a cube and vertically arranged on the electrode, the molecular area was 200 Å² and Γ was 330 pmol/cm² [6,32]. Table 1 shows that the molecular area and Γ were all lower than the aforementioned values. Therefore, alkanethiols of the same chain length can play supporting roles for the porphyrin ring and can be used as templates for porphyrin SAMs. For the porphyrins with short-chain lengths ($n = 3$), θ decreased with increasing Γ . Meanwhile, the molecular area also decreased with the self-assembly time of the alkanethiols when the template was increased. However, for porphyrins with long-chain lengths ($n = 12$), the change trend of Γ and the molecular area caused by the decreasing hindrance θ was not obvious. Comparing the two cases, the self-assembly adsorption of the long-chain alkanethiols was more difficult than that of the short-chain ones at the initial stage of adsorption. By contrast, the formation

Table 2

ET rate constants of porphyrins ($H_2TPPO(CH_2)_nSH$ ($n = 3, 12$)) with alkanethiols ($(CH_2)_nSH$, $n = 3, 12$) of the same chain length as the template.

| System | Time (h) | k_{ox} (mol ⁻¹ cm ³ s ⁻¹) | k_b (s ⁻¹) | k' (cm s ⁻¹) |
|----------|----------|---|--------------------------|----------------------------|
| $n = 3$ | 2 | 4.76×10^8 | 2.24×10^5 | 6.41×10^{-4} |
| | 4 | 1.27×10^8 | 1.22×10^5 | 4.66×10^{-4} |
| | 6 | 8.80×10^8 | 1.3×10^5 | 4.44×10^{-4} |
| | 8 | 2.35×10^8 | 0.7×10^5 | 2.71×10^{-4} |
| $n = 12$ | 2 | 1.60×10^{10} | 0.72×10^3 | 3.06×10^{-5} |
| | 4 | 3.72×10^{10} | 0.73×10^3 | 3.01×10^{-5} |
| | 6 | 2.97×10^{10} | 1.06×10^3 | 3.70×10^{-5} |
| | 8 | 2.41×10^{10} | 0.47×10^3 | 4.94×10^{-5} |

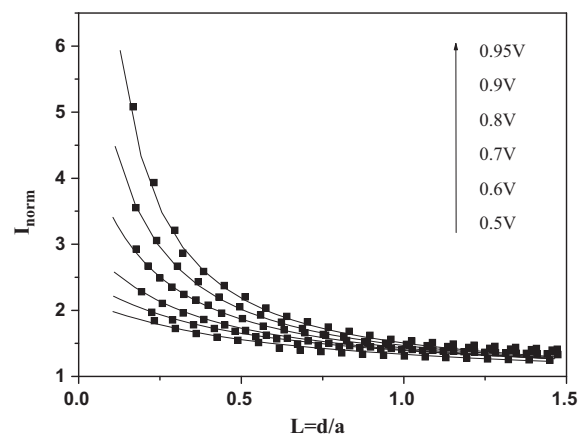


Fig. 2. Probe approach curves of totally Co porphyrins ($n = 12$) at different substrate potential in 0.1 M KCl solution. $E_{tip} = -0.1$ V vs Ag/AgCl, $\Gamma = 305$ pmol/cm².

of long-chain alkanethiol SAMs was easier than that of the short-chain ones. Thus, the long-chain porphyrins obtained the maximum θ at the initial stage of the self-assembly adsorption ($t = 2$ h), whereas the short-chain porphyrins obtained the maximum θ at the middle stage of the adsorption ($t = 4$ h). In addition, for the long-chain porphyrin SAMs ($n = 12$), the minimum molecular area and

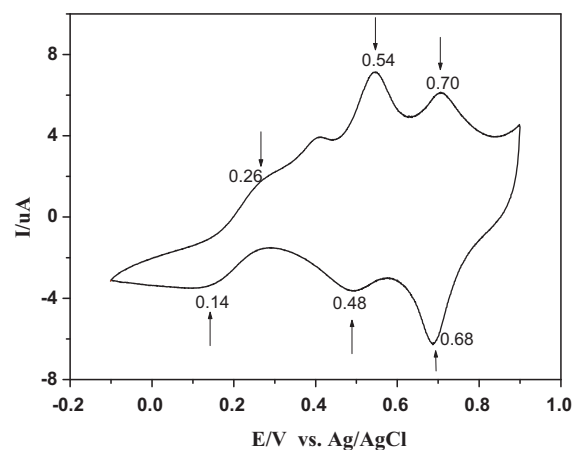


Fig. 3. The CVs of Co porphyrins ($n = 12$) in 1 mM $K_3Fe(CN)_6$ and 0.1 M KCl solution with scan rate of 100 mV/s.

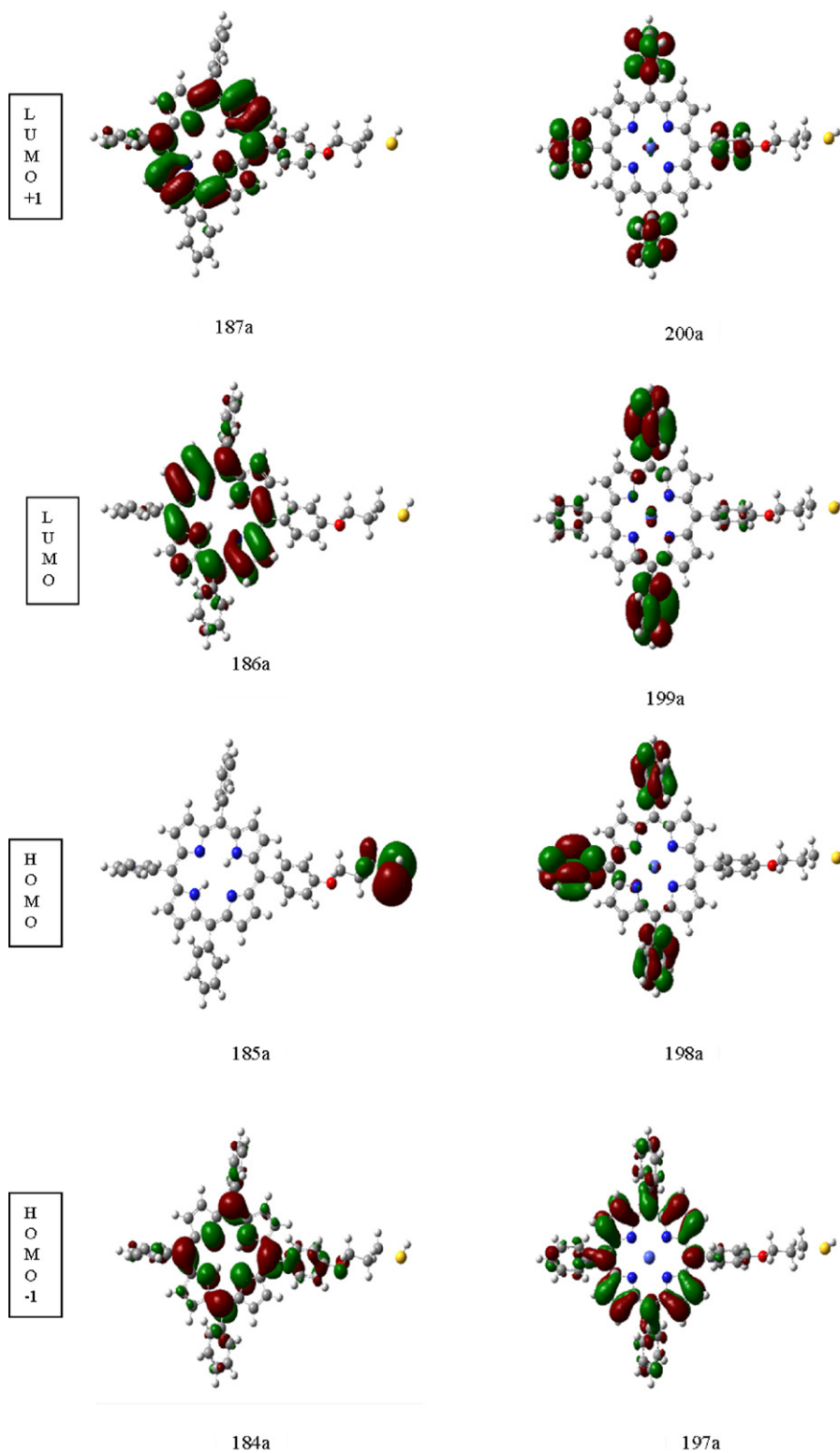


Fig. 4. Molecular electron cloud density and orbital energy calculation: left, $\text{H}_2\text{TPPO}(\text{CH}_2)_n\text{SH}$ ($n=3$), right, $\text{TPPO}(\text{CH}_2)_n\text{SH}-\text{Co}$ ($n=3$).

maximum Γ were obtained at the middle stage of the self-assembly adsorption ($t=4$ h), whereas for the short-chain porphyrins, the parameters varied with increasing self-assembly time. This phenomenon further demonstrates the effect of the chain length on the formation of SAMs at different stages of the self-assembly adsorption.

3.2. *ET constants of porphyrins with alkanethiol templates*

Sulfhydryl compounds were firmly bound to the gold electrode through the Au–S bond, and the high-order monolayer can spontaneously be formed on the electrode surface [46–50]. By considering porphyrin rings as the terminal group in SAMs as well as the

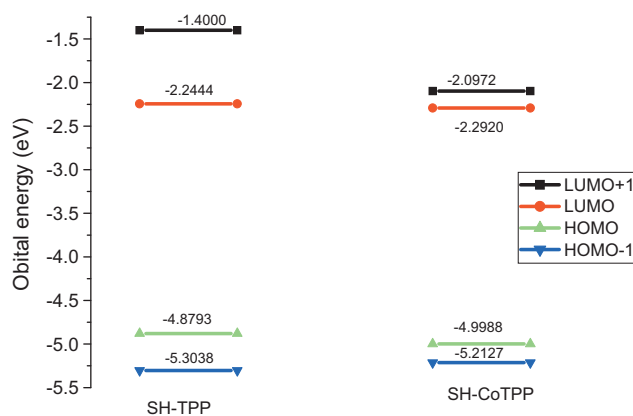


Fig. 4. (Continued).

presence of pinholes and defects on the surface of the electrode, the corresponding alkanethiol compounds with the same alkyl chain lengths were used as the templates on a substrate. In Scheme 3, two cases are presented: (a) porphyrins directly self-assembling on the substrate and (b) porphyrins self-assembling after the alkanethiol template has self-assembled on the substrate. The formation of porphyrin SAMs was disordered without the templates, but became highly order when alkanethiols were used as the templates. The values of the ET rate constant for the porphyrins with alkanethiols whose chain lengths are similar to those of the templates were calculated (Fig. 1). Table 2 shows the different ET rate constants obtained for the two cases. For the long-chain porphyrins ($n = 12$), k_{ox} reached a maximum value when the self-assembly time of the alkanethiols was short ($t = 4$ h). However, the k_{ox} for the short-chain porphyrins ($n = 3$) obtained its maximum value when the self-assembly time of the alkanethiols was increased ($t = 6$ h). This phenomenon strongly demonstrates the effect of the chain length on the structure of alkanethiols as the templates, and further affects the electron transport of porphyrin SAMs in the bimolecular reaction. The change trend may be attributed to the following reasons: (a) in the initial phase of the self-assembly adsorption, the short-chain alkanethiols can be adsorbed on the gold electrode better than the long-chain alkanethiols. The temporary disorders in the formation of the short-chain alkanethiols inadequately support the porphyrin ring at the short self-assembly adsorption time; (b) compared with the short-chain alkanethiols, the spacers containing long-chain alkanethiols exhibited better order on the gold electrode in the initial phase of the self-assembly adsorption. Under the same conditions, porphyrin compounds can insert the alkanethiol templates better. When the assembly time of alkanethiols is short, porphyrins with long-chain alkanethiols can be adsorbed at the absorptive site via self-assembly much easier than the short-chain ones; (c) the morphologies of the porphyrin rings with different alkyl chain lengths are different. That is, the orientation is parallel ($n = 3$) or perpendicular ($n = 12$) to the gold electrode, depending on the surface coverage (Γ) and the molecular areas [32,44,45]. In the presence of alkanethiols as the template, the arrangement of the porphyrin ring in SAMs can be perpendicular ($n = 12$) to the gold electrode, resulting in the accumulation of more porphyrin compounds on the electrode. In summary, as the template on the gold electrode, the alkanethiols significantly affected the ET process of the porphyrin compounds.

3.3. ET constants of porphyrins with Co metal inserted in the center of the porphyrin rings

Metalloporphyrin coordination compounds, such as vitamin B₁₂ (Co porphyrins), haemachrome (Fe porphyrins), and chlorophyll

(magnesium porphyrins) can undergo reversible redox interactions on the porphyrin rings or the central metal ion in natural processes [51]. The Co porphyrins have been chosen in the current study on a gold electrode because Co metal ion has the highest percentage of coordination under the same experimental conditions [52]. Fig. 2 shows the feedback curves of the metal (Co) porphyrins at the gold electrode with the substrate potential ranging from 0.5 V to 0.9 V. The experimental curves closely follow the theoretical ones, with a positive feedback at the substrate potential below 750 mV. These findings indicate that SAMs with metals exhibit no apparent blocking with the redox mediator, when the metal (Co) is inserted into the center of the porphyrin ring. The CVs of the metal porphyrins in 1 mM K₃Fe(CN)₆ and 0.1 M KCl solution are shown in Fig. 3. The three pairs of quasi-reversible peaks of Co porphyrins appeared, in with the first corresponding to the porphyrin ring, the second to the Co(II)–Co(III) bond and the third to Fe(CN)₆³⁻/Fe(CN)₆⁴⁻. The corresponding formal potentials were 700, 540 and 260 mV, respectively. Compared with the formal potential (700 mV) of porphyrins, the peak of the porphyrin rings in the metalloporphyrin shows a negative shift. Furthermore, the molecular electron cloud density and orbital energy of the highest occupied molecular orbital (HOMO) and lowest unoccupied molecular orbital LUMO were obtained using the DFT calculation shown in Fig. 4. The energy change in the HOMO and LUMO can cause the formal potential of porphyrin rings to shift negatively. Table 3 shows the ET rate constant of the Co porphyrin compounds with different alkyl chain lengths. Compared with those of the porphyrin compounds [32], the ET rate constants of the Co porphyrins clearly increased. The results are attributed to the following: (a) the changes in the orbital energy of HOMO and LUMO show that the insertion of the Co ion enhanced the electrochemical activity of the porphyrin rings to some extent; (b) the porphyrin ring underwent a small distortion from the coordination with the Co ion in its center, and the arrangement of porphyrins in SAMs became as loose as possible to facilitate the ET; (c) a comparison between the porphyrins and metalloporphyrins shows that an ET channel was added to provide for the insertion of the metal and dominate the ET pathway of metalloporphyrins [53].

Table 3

ET rate constants of Co-porphyrins with different alkyl chain lengths.

| System | k_{ox} (mol ⁻¹ cm ³ s ⁻¹) | k_b (s ⁻¹) | k' (cm s ⁻¹) |
|----------|---|--------------------------|----------------------------|
| $n = 3$ | 6.37×10^9 | 1.07×10^6 | 7.81×10^{-3} |
| $n = 12$ | 1.65×10^{11} | 4.77×10^4 | 9.65×10^{-4} |

4. Conclusions

Kinetic investigations on the two kinds of functional porphyrin SAMs on a gold electrode using SECM were completed. In both cases, the porphyrins were the focus of the study. Alkanethiols were prepared and used as the template on the gold electrode. The optimized self-assembly time of the alkanethiols was different for the two alkyl chains with different chain lengths. The template strongly affected the Γ and molecular area of the porphyrin compounds and significantly affected the ET kinetics of the porphyrins. In addition, the porphyrin SAMs were coordinated with the Co metal in the center of the porphyrin rings. In the presence of Co, the rate constant of ET clearly increased because of the changes in the orbital energy, the distortion of the porphyrin ring, and the existence of an additional ET channel.

Acknowledgments

This work was supported by the Natural Science Foundation of China (Nos. 20775060, 20875077 and 20927004), the Natural Science Foundation of Gansu (No. 0701RJZA109) and Key Projects of Scientific Research Base of Department of Education, Gansu Province (No. 08zx-07) of China.

Appendix A. Supplementary data

Supplementary data associated with this article can be found, in the online version, at [doi:10.1016/j.electacta.2012.01.049](https://doi.org/10.1016/j.electacta.2012.01.049).

References

- [1] I.O. Benitez, B. Bujoli, L.J. Camus, C.M. Lee, F. Odobel, D.R. Talham, *J. Am. Chem. Soc.* 124 (2002) 4363.
- [2] F.P. Zhi, X.Q. Lu, J.D. Yang, X.Y. Wang, H. Shang, S.H. Zhang, Z.H. Xue, *J. Phys. Chem. C* 113 (2009) 13166.
- [3] V. Chukharev, T. Vuorinen, A. Efimov, N.V. Tkachenko, *Langmuir* 21 (2005) 6385.
- [4] M.Y. Duan, J. Li, G. Mele, C. Wang, X.F. Lu, G. Vasapollo, F.X. Zhang, *J. Phys. Chem. C* 114 (2010) 7857.
- [5] Z.J. Zhang, S.F. Hou, Z.H. Zhu, Z.F. Liu, *Langmuir* 16 (2000) 537.
- [6] X.Q. Lu, L.M. Zhang, M.R. Li, X.Q. Wang, Y. Zhang, X.H. Liu, G.F. Zuo, *ChemPhysChem* 7 (2006) 854.
- [7] Z.J. Zhang, R.S. Hu, Z.F. Liu, *Langmuir* 16 (2000) 1158.
- [8] Z.J. Zhang, T. Imae, *Langmuir* 17 (2001) 4564.
- [9] S.Z. Zou, R.S. Clegg, F.C. Anson, *Langmuir* 18 (2002) 3241.
- [10] G. Li, T. Wang, A. Schulz, S. Bhosale, M. Lauer, P. Espindola, J. Heinze, J.H. Fuhrhop, *Chem. Commun.* 5 (2004) 552.
- [11] J.C. Love, L.A. Estroff, J.K. Kriebel, R.G. Nuzzo, G.M. Whitesides, *Chem. Rev.* 105 (2005) 1103.
- [12] N. Phares, R.J. White, K.W. Plaxco, *Anal. Chem.* 81 (2009) 1095.
- [13] S.Q. Lud, S. Neppel, G. Richter, P. Bruno, D.M. Gruen, R. Jordan, P. Feulner, M. Stutzmann, J.A. Garrido, *Langmuir* 26 (2010) 15895.
- [14] M. Chirea, A. Cruz, C.M. Pereira, A.F. Silva, *J. Phys. Chem. C* 113 (2009) 13077.
- [15] S. Sek, A. Misicka, R. Bilewicz, *J. Phys. Chem. B* 104 (2000) 5399.
- [16] W. Tu, K. Takai, K. Fukui, A. Miyazaki, T. Enoki, *J. Phys. Chem. B* 107 (2003) 10134.
- [17] M. Kozaki, K. Akita, K. Okada, *Org. Lett.* 9 (2007) 1509.
- [18] T.H. Xu, R. Lu, X.L. Liu, X.Q. Zheng, X.P. Qiu, Y.Y. Zhao, *Org. Lett.* 9 (2007) 797.
- [19] Y. Morishima, H. Aota, K. Saegusa, M. Kamachi, *Macromolecules* 29 (1996) 6505.
- [20] J.P. Yang, P.C. Huang, *J. Appl. Polym. Sci.* 77 (2000) 484.
- [21] L.J. Zhu, J. Wang, T.G. Reng, G.Y. Li, D.C. Guo, C.C. Guo, *J. Phys. Org. Chem.* 23 (2010) 190.
- [22] S. Kang, T. Umeyama, M. Ueda, Y. Matano, H. Hotta, K. Yoshida, S. Isoda, M. Shiro, H. Imahori, *Adv. Mater.* 18 (2006) 2549.
- [23] F. Zhang, V. Roznyatovskiy, F.F. Fan, V. Lynch, J.L. Sessler, A.J. Bard, *J. Phys. Chem. C* 115 (2011) 2592.
- [24] M.A. Mezzour, R. Cornut, E.M. Hussien, M. Morin, J. Mauzeroll, *Langmuir* 26 (2010) 13000.
- [25] A.J. Bard, M.V. Mirkin, P.R. Unwin, D.O. Wipf, *J. Phys. Chem.* 96 (1992) 1861.
- [26] P.R. Unwin, A.J. Bard, *J. Phys. Chem.* 95 (1991) 7814.
- [27] M.V. Mirkin, B.R. Horrocks, *Anal. Chim. Acta* 406 (2000) 119.
- [28] R. Martin, P.R. Unwin, *Anal. Chem.* 70 (1998) 276.
- [29] W.T. Wang, D.L. Shan, Y. Yang, C.C. Wang, Y.Q. Hu, X.Q. Lu, *Chem. Commun.* 47 (2011) 6975.
- [30] X.Q. Lu, P. Sun, D.N. Yao, B.W. Wu, Z.H. Xue, X.B. Zhou, R.P. Sun, L. Li, X.H. Liu, *Anal. Chem.* 82 (2010) 8598.
- [31] X.Q. Lu, T.X. Wang, X.B. Zhou, Y. Li, B.W. Wu, X.H. Liu, *J. Phys. Chem. C* 115 (2011) 4800.
- [32] W.T. Wang, X.J. Li, X.Y. Wang, H. Shang, X.H. Liu, X.Q. Lu, *J. Phys. Chem. B* 114 (2010) 10436.
- [33] Q. Wang, F.P. Zhi, W.T. Wang, X.H. Xia, X.H. Liu, F.F. Meng, Y.Y. Song, C. Yang, X.Q. Lu, *J. Phys. Chem. C* 113 (2009) 9359.
- [34] G.F. Zuo, X.H. Liu, J.D. Yang, X.J. Li, X.Q. Lu, *J. Electroanal. Chem.* 605 (2007) 81.
- [35] X.Q. Lu, B.Q. Lv, Z.H. Xue, M. Zhang, Y.S. Wang, J.W. Kang, *Anal. Lett.* 35 (2002) 1811.
- [36] N. Nishimura, M. Ooi, K. Shimazu, J.H. Fu, K.J. Uosaki, *Electroanal. Chem.* 473 (1999) 75.
- [37] M. Tsionsky, J.F. Zhou, S. Amemiya, F.-R.F. Fan, A.J. Bard, *Anal. Chem.* 71 (1999) 4300.
- [38] Y. Shao, M.V. Mirkin, *J. Phys. B* 102 (1998) 9915.
- [39] F. Forouzan, A.J. Bard, M.V. Mirkin, *Isr. J. Chem.* 37 (1997) 155.
- [40] L. Biao, A.J. Bard, M.V. Mirkin, S.E. Creager, *J. Am. Chem. Soc.* 126 (2004) 1485.
- [41] A. Kiani, M.A. Alpuche-Aviles, P.K. Eggers, M. Jones, J.J. Gooding, M.N. Paddon-Row, A.J. Bard, *Langmuir* 24 (2008) 2841.
- [42] X.Q. Lu, F.P. Zhi, H. Shang, X.Y. Wang, Z.H. Xue, *Electrochim. Acta* 601 (2007) 10.
- [43] C.H. Hamann, A. Hamnett, W.V. Weinheim, *Electrochemistry*, Wiley-VCH, New York, Chichester, Brisbane, Singapore and Toronto, 1998.
- [44] D.B. Robinson, E.D. Chidsey, *J. Electroanal. Chem.* 438 (1997) 121.
- [45] H. Imahori, H. Norieda, S. Ozawa, *Langmuir* 14 (1998) 5335.
- [46] A. Ulman, *Chem. Rev.* 96 (1996) 1533.
- [47] J.M. Tour, L. Jones, D.L. Pearson, J.J.S. Lamba, T.P. Burgin, G.M. Whitesides, D.L. Allara, A.N. Parikh, S. Atre, *J. Am. Chem. Soc.* 117 (1995) 9529.
- [48] M.H. Zareie, H. Ma, B.W. Reed, A.K.Y. Jen, M. Sarikaya, *Nano Lett.* 3 (2003) 139.
- [49] Y. Xia, G.M. Whitesides, *Angew. Chem. Int. Ed.* 37 (1998) 550.
- [50] Z.F. Liu, K. Hashimoto, A. Fujishima, *Nature* 347 (1990) 658.
- [51] D. Jones, A.S. Hinman, *Dalton Trans.* 21 (1992) 1503.
- [52] M.K. Geno, J. Halpern, *J. Am. Chem. Soc.* 109 (1987) 1238.
- [53] X.Q. Lu, M.R. Li, C.H. Yang, L.M. Zhang, L. Jiang, H.X. Li, L. Jiang, C.M. Liu, W.P. Hu, *Langmuir* 22 (2006) 3035.